Provided for non-commercial research and education use.
Not for reproduction, distribution or commercial use.

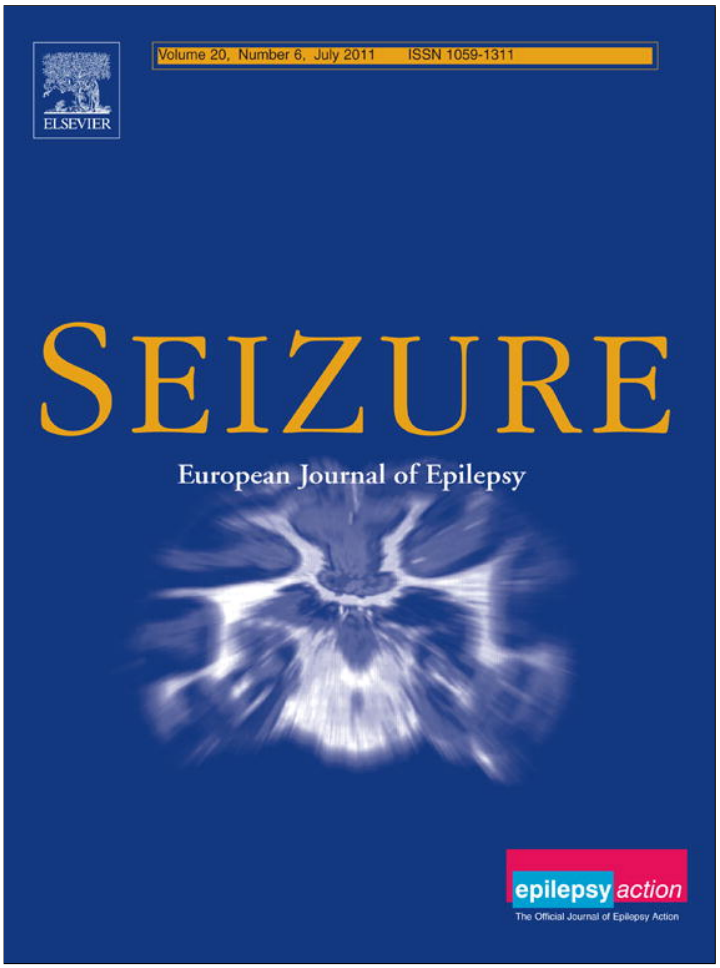

This article appeared in a journal published by Elsevier. The attached copy is furnished to the author for internal non-commercial research and education use, including for instruction at the authors institution and sharing with colleagues.

Other uses, including reproduction and distribution, or selling or licensing copies, or posting to personal, institutional or third party websites are prohibited.

In most cases authors are permitted to post their version of the article (e.g. in Word or Tex form) to their personal website or institutional repository. Authors requiring further information regarding Elsevier's archiving and manuscript policies are encouraged to visit:

http://www.elsevier.com/copyright

Author's personal copy

Seizure 20 (2011) 449–457

Contents lists available at ScienceDirect

Seizure

journal homepage: www.elsevier.com/locate/yseiz

Localization of ictal onset zones in Lennox-Gastaut syndrome using directional connectivity analysis of intracranial electroencephalography

Young-Jin Jung [a,1], Hoon-Chul Kang [b,1], Keom-Ok Choi [b], Joon Soo Lee [b], Dong-Seok Kim [c], Jae-Hyun Cho [a], Shin-Hye Kim [b], Chang-Hwan Im [d,*], Heung Dong Kim [b,**]

[a] Department of Biomedical Engineering, Yonsei University, Wonju, Kangwon-do, Republic of Korea
[b] Department of Pediatrics, Severance Children's Hospital, Epilepsy Research Institute, Yonsei University College of Medicine, Seoul, Republic of Korea
[c] Department of Neurosurgery, Severance Hospital, Yonsei University College of Medicine, Seoul, Republic of Korea
[d] Department of Biomedical Engineering, Hanyang University, 17 Haengdang-dong, Seongdong-gu, Seoul, 133-791, Republic of Korea

ARTICLE INFO

Article history:
Received 1 November 2010
Received in revised form 1 February 2011
Accepted 7 February 2011

Keywords:
Ictal onset zone
Lennox-Gastaut syndrome (LGS)
Directional connectivity analysis
Directed transfer function (DTF)
Intracranial electroencephalography (iEEG)
Ictal epileptiform activity

ABSTRACT

Introduction: Neuroscientists are becoming interested in the application of computational EEG analysis to the identification of ictal onset zones; however, most studies have focused on the localization of ictal onset zones in focal epilepsy. The present study aimed to estimate the ictal onset zone of Lennox-Gastaut syndrome (LGS) with bilaterally synchronous epileptiform discharges from intracranial electroencephalography (iEEG) recordings using directional connectivity analysis.
Methods: We analyzed ictal iEEG data acquired from three LGS patients who underwent epileptic surgery with favorable surgical outcomes. To identify the ictal onset zones, we estimated the functional directional connectivity network among the intracerebral electrodes using the directed transfer function (DTF) method.
Results: The analysis results demonstrated that areas with high average outflow values corresponded well with the surgical resection areas identified using electrophysiologic data and conventional neuroimaging modalities.
Discussions: Our results suggest that the DTF analysis can be a useful auxiliary tool for determining surgical resection areas prior to epilepsy surgery in LGS patients. This is the first research article demonstrating that directional connectivity analysis of iEEG recording data can be used for delineating surgical resection areas in generalized epilepsy patients who need surgical treatment.
© 2011 British Epilepsy Association. Published by Elsevier Ltd. All rights reserved.

1. Introduction

Precise identification of ictal onset zones in patients with intractable drug-resistant epilepsy is of great importance for successful epilepsy surgery. To estimate ictal onset zones, various neurophysiologic and neuroimaging modalities have been utilized such as video-monitored scalp electroencephalography (EEG), magnetoencephalography (MEG), ictal/interictal single photon emission computed tomography (SPECT), positron emission tomography (PET), and functional magnetic resonance imaging (fMRI) triggered by simultaneously recorded EEG.[1–4] However, despite the recent rapid developments in brain imaging technology, the noninvasive imaging modalities listed above have not been directly used to localize the surgical resection areas, but have been used as supplementary tools to determine the locations of intracranial EEG (iEEG) electrodes, because of the relatively limited spatial resolutions of these tools. Indeed, in modern clinical neurophysiology, information obtained from iEEG recordings is regarded as the gold standard for pre-surgical evaluation prior to epilepsy surgery. Traditionally, ictal onset zones have been identified visually by well-experienced electroencephalographers. For example, ictal onset zones are usually found in locations with sustained rhythmic changes on electrocorticograms (ECoG) accompanied by subsequent clinically typical seizure activity.

Recently, neuroscientists have become interested in the application of computational EEG analysis methods to the identification of ictal onset zones and epileptic networks, due to the rapid development in digital EEG systems and computational neuroscience. To identify ictal onset zones, various functional connectivity measures have been adopted, such as mutual

* Corresponding author at: Department of Biomedical Engineering, Hanyang University, 17 Haengdang-dong, Seongdong-gu, Seoul, 133-791, Republic of Korea. Tel.: +82 2 2220 2322; fax: +82 2 2296 5943.
** Corresponding author at: Department of Pediatrics, Pediatric Epilepsy Clinics, Severance Children's Hospital, Epilepsy Research Institute, Yonsei University College of Medicine, 134 Shinchon-dong, Seodaemun-gu, Seoul 120-752, Republic of Korea. Tel.: +82 2 2228 1703; fax: +82 2 2626 1249.
E-mail addresses: ich@hanyang.ac.kr (C.-H. Im), hdkimmd@yuhs.ac (H.D. Kim).
[1] These authors contributed equally to this work.

1059-1311/$ – see front matter © 2011 British Epilepsy Association. Published by Elsevier Ltd. All rights reserved.
doi:10.1016/j.seizure.2011.02.004

Author's personal copy

information,[5] stochastic qualifiers,[6] and directed transfer functions (DTFs).[7,8] Functional connectivity analysis methods have been shown to be useful tools in revealing the underlying mechanisms of epileptic networks. Among various indices to measure functional connectivity between neural signals, DTF has attracted the most attention as it can efficiently estimate causal interactions among multiple EEG signals in the frequency domain.

Since Kaminski and Blinowska's first report in the early 1990s,[9] DTF has been applied extensively to the analysis of epileptic networks. Series of studies have demonstrated that the DTF technique can be used to identify ictal onset zones from iEEG recordings, specifically in mesial temporal lobe epilepsy,[10] lateral temporal lobe epilepsy,[11] and neocortical extra-temporal lobe epilepsies.[12,13] The DTF-based approach has been combined with EEG-based or ECoG-based source localization methods,[7,14] as well as with single-class support vector machine (SVM) algorithms,[8] providing novel modalities for localizing ictal onset zones.

Despite extensive studies on DTF-based ictal onset zone localization,[7,10–14] however, all of the previous studies have focused only on the localization of ictal onset zones in focal epilepsy. However, in some patients with generalized epilepsy such as Lennox-Gastaut syndrome (LGS), localization of ictal onset zones is also critical for surgical treatment. LGS is described as an epileptic syndrome with intractable, multiple seizure types including tonic, atonic, myoclonic and atypical absence seizures. Its interictal EEG pattern is characterized by interictal bilaterally synchronous slow spike-waves and paroxysmal fast activity.[15] Some patients with LGS have focal lesions that attribute to secondary generalized epileptic encephalopathy; these focal lesions are generally identified via EEG, MRI, and other functional neuroimaging techniques. Because of their generalized ictal iEEG discharges, however, surgical resection areas are usually determined based on their interictal characteristics on iEEG, with the help of advanced neuroimaging techniques. Recent studies reported successful outcomes of resective epilepsy surgery for children with LGS, despite abundant generalized and multiregional EEG abnormalities.[16,17] However, additional refinement techniques to confirm the locations of ictal onset zones are still required. In the present study, we localized ictal onset zones in three LGS patients by applying the DTF method to ictal iEEG recordings obtained before epilepsy surgery and investigated the feasibility of using the DTF method for pre-surgical evaluation of LGS.

2. Subjects and methods

2.1. Subjects

Of 27 patients who had LGS and underwent resective pediatric epilepsy surgery at Severance Children's Hospital during 2001–2007, we identified 16 patients who became seizure free after focal resective surgery. Then we excluded patients who had cerebral infarctions or progressive underlying metabolic diseases or chromosomal anomalies. Finally three patients were selected and all clinical data, including iEEG recordings, were obtained from them. This study was conducted under the permission from the institutional review boards of Severance Hospital. Parents or guardians of all subjects were asked to provide a written consent before their child's data were enrolled in the study.

The first subject (LYS) was a 3-year-old boy with severe mental impairment (Intelligence Quotient (IQ) of 25) who had suffered from refractory epilepsy since 7 months of age. Two types of seizures were observed in this subject, generalized tonic spasms and head drops, and none of the available antiepileptic medications could suppress his seizures. In this patient's pre-surgical evaluation at the age of 3 years, the MRI findings were normal. FDG-PET scans did not reveal any asymmetric hypometabolism, but SISCOM, which was obtained using a slow ictal SPECT injection protocol, lateralized consistently to the right frontotemporal area with an epileptogenic focus. Continuous video EEG monitoring showed frequent generalized slow spikes and waves and generalized paroxysmal fast activities, as well as localized epileptiform discharges or bisynchronous sharp waves predominantly located in the right frontotemporal areas. Ictal EEG showed generalized slow waves followed by low-voltage fast activities during generalized tonic seizures or head drops, but did not aid in the lateralization of the epileptogenic area. Based on the results of a Phase I study and ictal/interictal iEEG monitoring, the patient underwent a right frontal resection at 3 years of age and was free of seizures for 2.5 years before his seizures recurred at 6 years of age. The posterior margin of the pre-resection site was further resected, and the patient has been free of seizures for 1.6 years (see Fig. 2b for the final resection areas marked on the electrode grids). Pathologic result was classified as focal cortical dysplasia (CD) type. The EEG after reoperation showed nearly normalized background activities and no epileptiform discharge.

The second subject (JMS) was a 2-year-old boy with severe mental impairment, who had suffered from refractory epilepsy since 5 months of age. Seizures presented as head drops and atypical absences and were intractable to several available antiepileptic medications. Brain MRI showed a blurring of the gray-white matter interface on the right frontal area. FDG-PET scans did not reveal any asymmetric hypometabolism, and slow ictal SPECT injection was unsuccessful. Slow ictal SPECT injection means infusion of ^{99m}Tc-ethyl cysteinate dimer at a regular velocity throughout 2 min from the first repetitive spasms by continuous injection. Continuous video EEG monitoring consistently showed abundant generalized slow spikes and waves and generalized paroxysmal fast activities, as well as localized epileptiform discharges in the right frontal area. Ictal EEG showed generalized slow waves followed by electrodecremental fast activities during head drops, but did not aid in the lateralization of the epileptogenic area. According to the results of a Phase I study and ictal/interictal iEEG monitoring, the right frontal area and right anterior temporal lobe (see Fig. 3b for the resection area) were resected during surgery. This patient has been free of seizures for 5.6 years without medication. The pathologic result was classified as focal CD type. The EEG after operation revealed nearly normalized background activities only with occasional multifocal sharp waves.

The third subject (SWJ) was a 3-year-old boy with severe mental impairment (IQ of 29) who had developed refractory epilepsy at 18 months of age. This patient presented with two types of seizures, generalized tonic spasms and staring spells, which available antiepileptic medications were not able to suppress. The MRI findings for pre-surgical evaluation when the patient was 3 years old showed suspicious but not definite cortical thickening on the right frontal area. FDG-PET also revealed focal hypometabolism on the right frontal lobe and SISCOM, which was obtained via a slow ictal SPECT injection protocol, lateralized consistently to the right frontotemporal area with an epileptogenic focus. Continuous video EEG monitoring showed frequent generalized slow spikes and waves and generalized paroxysmal fast activities and localized epileptiform discharges or bisynchronous sharp waves in the right frontotemporal areas. Ictal EEG showed generalized slow waves followed by low-voltage fast activities during generalized tonic seizures, but did not aid in the lateralization of the epileptogenic area. Based on the results of a Phase I study and ictal/interictal iEEG monitoring, the patient underwent a right frontal resection when he was 3 years old, which reduced the frequency of his seizures but did not control them completely. The right inferior frontal gyrus and right temporal area were further resected, and this subject has been free of seizures for 1.6 years on a reduced number of medications (see Fig. 4b for the

Author's personal copy

final resection areas marked on the electrode grids). Pathologic result was classified as focal CD type. The EEG after reoperation revealed nearly normalized background activities and no epileptiform discharge.

2.2. Determination of surgical resection area

We used a variety of neuroimaging modalities to determine the surgical area. All patients were examined using a video-EEG monitoring system with electrodes placed according to the international 10–20 system to define a semiology of habitual seizures and to identify epileptogenic foci. Epileptogenic areas were delineated primarily through interpretation of EEG data, and other imaging modalities were used to reinforce these findings. Intracranial EEG monitoring using subdural electrodes was also used to determine surgical resective margins. Preoperative and intraoperative functional mapping and intraoperative ECoG were also performed when necessary.[18,19]

Standard MRI was performed with conventional spin-echo T1-weighted sagittal, T2-weighted axial, flair axial, oblique coronal, and flair oblique coronal sequences, as well as with ultrafast gradient echo T1-weighted 3D coronal sequences. A Philips MRI Achieva 3.0 T Release 2.5.3.3 (USA) was used to acquire seizure-specialized sequences, termed seizure phase I images, in accordance with the protocol described in our previous study.[18]

PET images were acquired using a GE ADAVANCE scanner (GE, Milwaukee, WI, USA) in 3D mode. The transaxial resolution of the system was 5.2 mm full-width-half-maximum (FWHM) at the center of the field of view (FOV). Approximately 5 mCi of 18F-FDG was injected intravenously. The emission scan began 40 min after injection and lasted 15 min, and an 8 min transmission scan was subsequently acquired for the purpose of attention correction.

To acquire SISCOM images, ictal SPECTs were obtained through the prolonged continuous slow injection of a ^{99m}Tc-ethyl cysteinate dimer (ECD) when the observer detected the first ictal spasm of a cluster. Prolonged continuous slow injection refers to infusion via continuous injection at a regular velocity for 2 min from the onset of the first repetitive brief seizures. At least three habitual brief tonic spasms or head drops were recorded during injection of ECD. SISCOM images were constructed using a UNIX-based workstation with image-analysis software packages (ANALYZE 7.5 and Analyze/AVW; Biomedical Imaging Resource, Mayo Clinic Foundation, Rochester, MN, USA).

The surgical area was defined based on the clinical, neuroimaging, and electrophysiological results. The resection margin for epilepsy of a neocortical origin was defined by (1) the presence of either a discrete lesion on MRI and functional neuroimages compatible with ictal or interictal intracranial EEG, (2) various interictal intracranial EEG findings including >3 repetitive spikes per second, runs of repetitive spike and slow wave discharges, localized or spindle-shaped fast activities and electrodecremental fast activities, and (3) the absence of an eloquent cortex. The diagnosis and classification of pathologic CD were made according to the system of Palmini et al.[20]

2.3. iEEG data acquisition

In all patients, ictal iEEG data were recorded using a multichannel digital EEG acquisition system (Telefactor, Grass Technologies) at a sampling rate of 200 Hz. The locations of the grid and strip subdural electrodes were determined based on the multimodal neuroimaging results, as described in the previous section (see Figs. 2b, 3b, and 4b for the grid and strip electrode locations). The recorded iEEG data were reviewed by an epileptologist, and 16 to 19 seizures were observed per subject. Seizure onset times were identified visually by the epileptologist with the aid of video monitoring. Fig. 1a shows an example of the ictal iEEG signals recorded at 104 electrodes from a single subject (LYS); these signals are segmented with respect to the ictal onset time centered at 5 sec. No specific pre-processing procedures except for baseline correction and 60 Hz notch filtering were applied to the raw iEEG data.

2.4. Localization of ictal onset zone with the DTF method

Digital iEEG recordings from three LGS patients were analyzed using the DTF method[9] to localize the ictal onset zone. The DTF method has been demonstrated to be a useful tool for the analysis of causal interactions among several signals over various frequency bands, and the procedures have been described in detail in previous studies.[9,21] DTF is formulated in the framework of the multivariate autoregressive (MVAR) model.[22–25] In the framework of the MVAR model, a multivariate process can be described as a data vector X of M source signals: $X(t) = (X_1(t), X_2(t), \ldots, X_M(t))^{\mathrm{T}}$. The MVAR model can then be constructed as

$$X(t) = \sum_{n=1}^{p} A_n X(t-n) + E(t), \tag{1}$$

where $E(t)$ represents a vector composed of white noise values at time t, A_n is an $M \times M$ matrix composed of the model coefficients, and p is the model order. In the present study, the model order was determined by means of criteria derived using the Bayesian information criterion (BIC).[26] The BIC generally penalizes free parameters more strongly than does the Akaike information criteria,[23] thereby preventing over-fitting due to excessively large model orders. Average model orders for subjects LYS, JMS, and SWJ were 5.55 ± 1.10, 4.44 ± 1.09, and 8.05 ± 1.08, respectively. We also assured that slight changes in model order (± 1) did not influence the resultant DTF patterns. The MVAR model was then transformed into the frequency domain as follows:

$$X(f) = A^{-1}(f)E(f) = H(f)E(f), \tag{2}$$

where f denotes a specific frequency and the $H(f)$ matrix is the so-called transfer matrix, which is defined as

$$H(f) = A^{-1}(f) = \left(\sum_{n=0}^{p} A_n e^{-i2\pi f n \Delta t} \right)^{-1}, \quad A_0 = -I, \tag{3}$$

where I is an identity matrix.

The DTF was defined in terms of the elements of the transfer matrix H_{ij} as

$$\gamma_{ij}^2(f) = \frac{|H_{ij}(f)|^2}{\sum_{m=1}^{k} |H_{im}(f)|^2}, \tag{4}$$

where $\gamma_{ij}(f)$ denotes the ratio between inflow from signal j to signal i and all inflows to signal i, and k is the number of signals. The DTF ratio ranges between 0 and 1, with values close to 1 indicating that signal i is caused by signal j. In contrast, values close to 0 indicate that there is no information flow from signal j to signal i at a specific frequency.

To determine the frequency band of interest, the time-domain iEEG signals were transformed into frequency domains using the short-time Fourier transform (STFT). For the STFT calculation, we used a "spectrogram" function implemented in Matlab (ver. 7.8, Mathworks Inc., USA). The analysis window used for the STFT calculation was the Kaiser window with 256 data samples, an 80% overlap rate, and a beta value of 5.

Fig. 1 shows an example of the time-frequency spectrogram (Fig. 1b) obtained from an ictal event of a subject's (LYS) iEEG data (Fig. 1a), where the ictal onset time was centered at 5 s. We observed distinct increases in the spectral power around the ictal

Author's personal copy

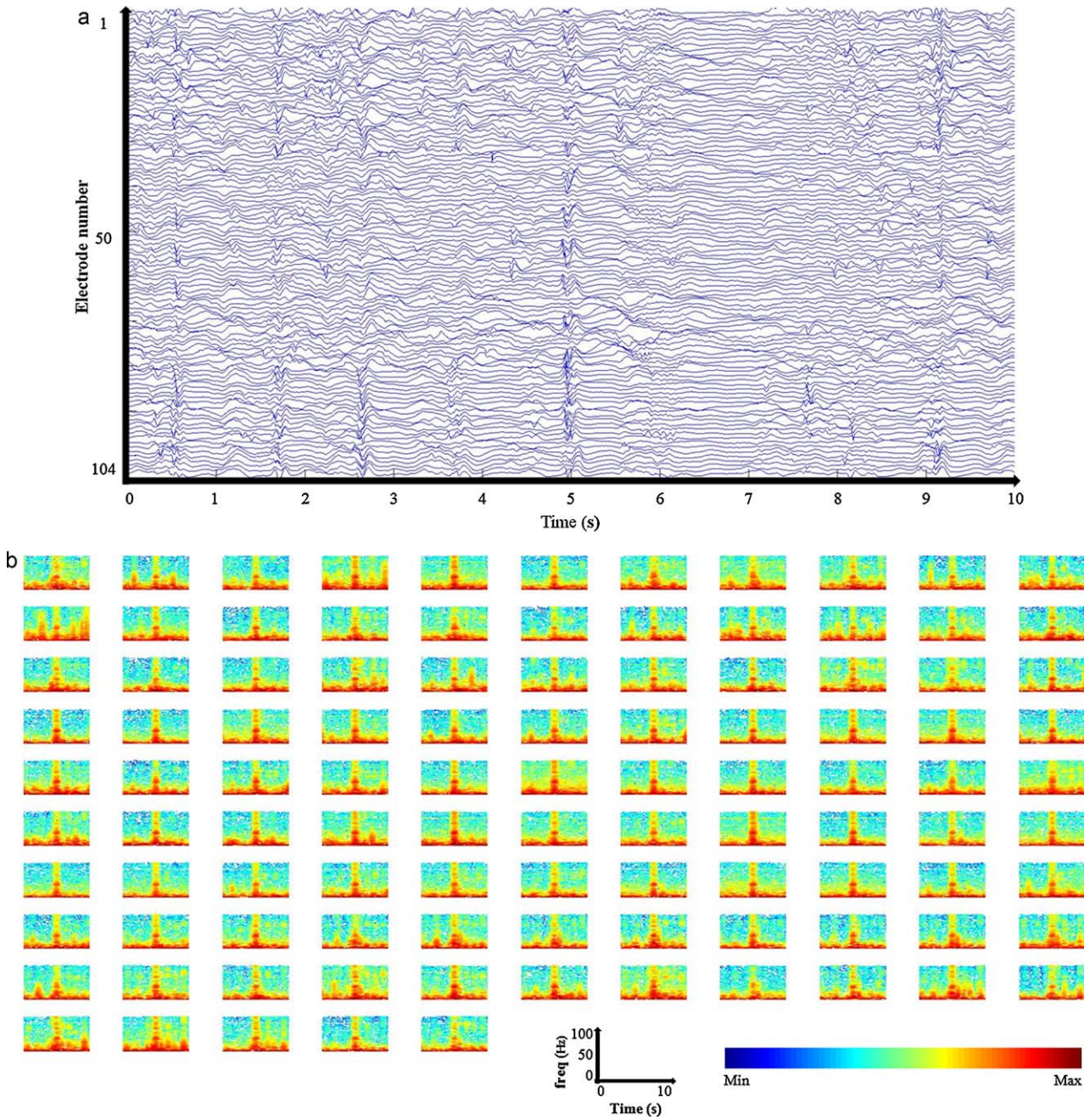

Fig. 1. An example of ictal iEEG signals and a time-frequency spectrogram (an ictal event of subject 1): (a) Ictal iEEG data recorded from subdural grids and strips during 10 s. The ictal onset time was 5 s. (b) Time-frequency spectrograms estimated for 104 subdural electrodes. Values in the spectrogram were normalized with respect to the maximum. The spectrograms were used to determine the frequency bands of interest. Distinct changes in spectral power can be observed around the ictal onset time, covering the entire alpha, beta, and gamma frequency bands.

onset time in most iEEG channels. The frequency band that showed distinct changes in spectral power was very broad, covering approximately the entire alpha, beta, and gamma frequency bands. Similar changes were observed in all ictal events of the three patients. Based on the time-frequency analysis, we determined the frequency band of interest (FOI) to be 8–50 Hz for all subjects. We confirmed through several simulations that the bandwidth of FOI had a negligible influence on the DTF analysis results, even when the FOI was restricted to only the alpha frequency band (8–12 Hz).

We then evaluated the DTF values for each ictal event. We set the analysis time window to 800 time samples (4 s) centered at each ictal onset time, considering the duration of the ictal events. We also confirmed that different window sizes ranging from 3.5 s to 5 s did not influence the resultant outflow patterns. The DTF values $\gamma_{ij}(f)$ were then averaged over the FOI (8–50 Hz in the present study), resulting in a single value, denoted as τ_{ij}, between a pair of signals i and j.

To quantify the extent to which an individual signal affects the generation of other signals, the averaged outflow of an ith signal was evaluated as

$$OF_i = \frac{1}{k-1} \sum_{\substack{j=1 \\ j \neq i}}^{k} \tau_{ji}, \tag{5}$$

Author's personal copy

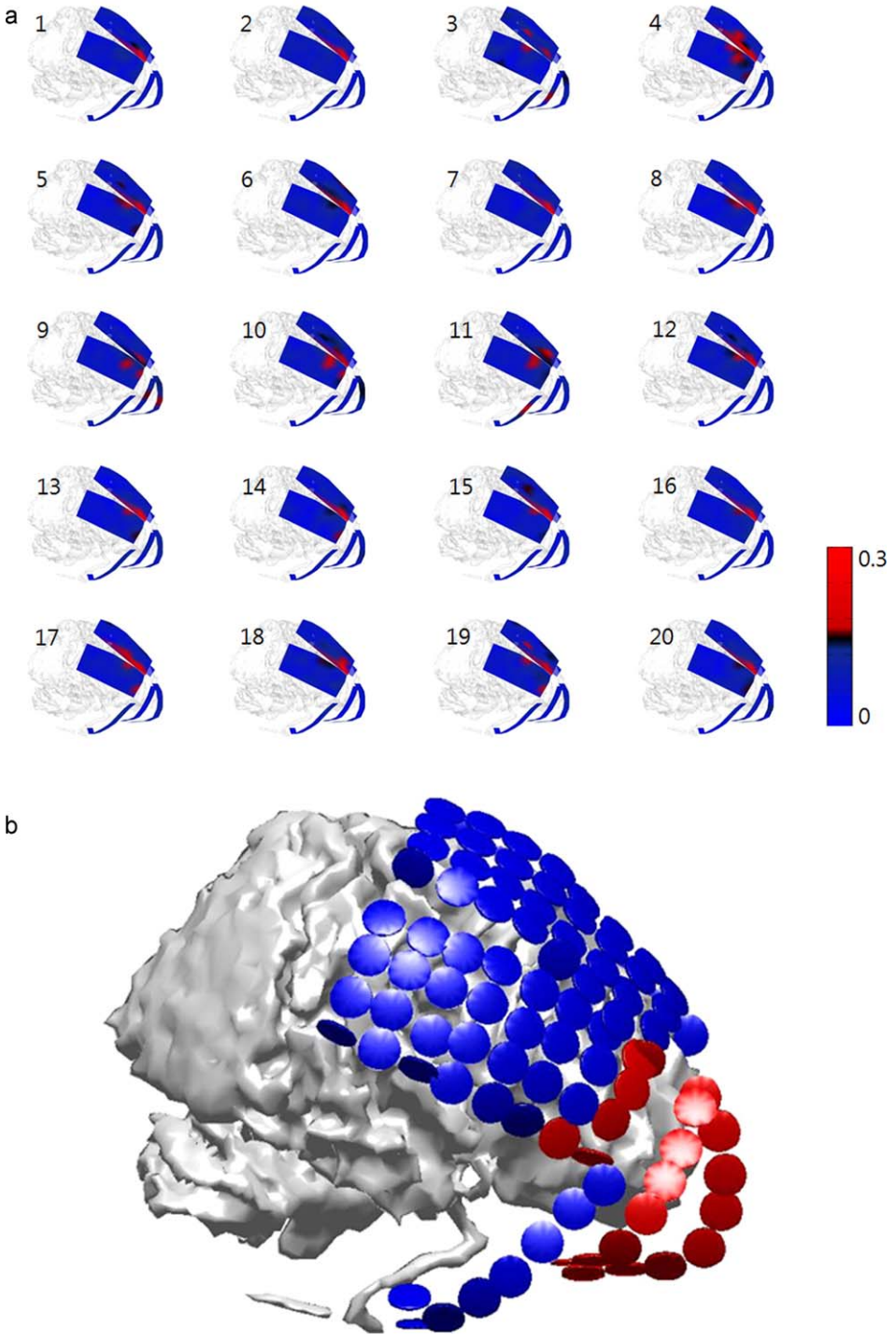

Fig. 2. The distributions of outflow values calculated for subject 1: (a) 3D outflow maps estimated for 20 ictal events; (b) the surgical resection areas (red color) marked on subdural electrodes. Numbers in (a) represent the event number. (For interpretation of the references to color in this figure legend, the reader is referred to the web version of the article.)

where k is the number of signals. Similarly, the averaged inflow of the ith signal can be evaluated as

$$IF_i = \frac{1}{k-1} \sum_{\substack{j=1 \\ j \neq i}}^{k} \tau_{ij}. \quad (6)$$

However, we did not use this measure in the present study, as outflow values can localize ictal signal generators better than can inflow values.[11,13] Zones with higher outflow values can be regarded as probable ictal onset zones. All of the above processes were performed using in-house software coded with Matlab.

After evaluating the outflow value for each iEEG signal, the distributions of the outflow values were illustrated on 3D brain images (see Fig. 2). The cortical surface model was generated from the individual T1-weighted MR images using CURRY6 for Windows (Compumedics Inc., USA). The locations of the subdural electrodes were obtained from the individual CT images and were registered on the segmented cortical surface model semi-automatically using the same software. The resultant outflow maps were generated

Author's personal copy

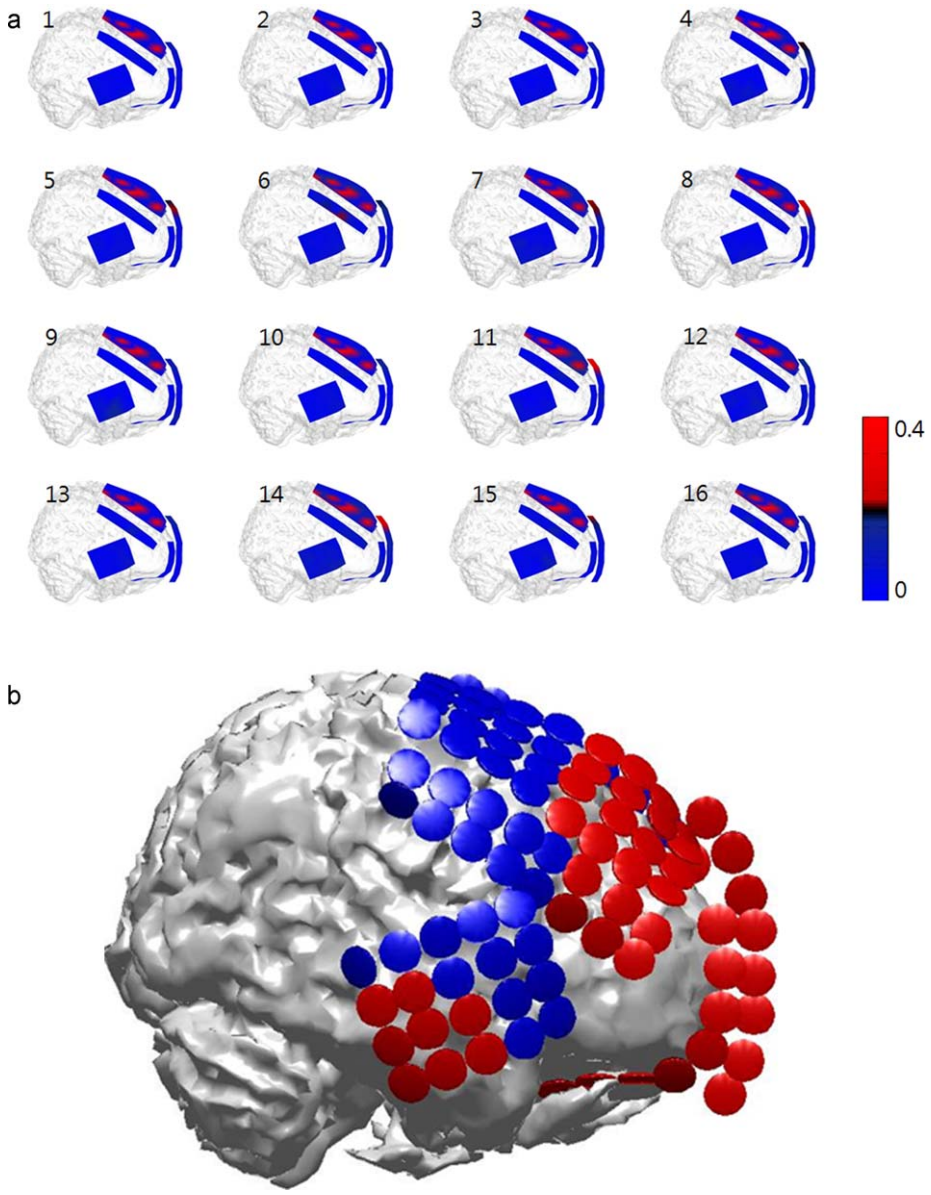

Fig. 3. The distributions of outflow values calculated for subject 2: (a) 3D outflow maps estimated for 16 ictal events; (b) the surgical resection areas (red color) marked on subdural electrodes. Numbers in (a) represent the event number. (For interpretation of the references to color in this figure legend, the reader is referred to the web version of the article.)

using Matlab. Finally, the estimated ictal onset zones were compared with the surgical resection areas of each LGS patient.

3. Results

We first estimated the DTF values of the iEEG signals recorded from the three LGS patients and then overlayed the averaged outflow values defined in (5) on each subject's 3D anatomical images. Fig. 2 shows the distributions of the outflow values evaluated for subject 1 (LYS), as well as the surgical resection area marked on the subdural electrodes. In this case, 20 ictal events measured from 104 electrodes were analyzed. The 3D outflow maps depicted in Fig. 2a consistently showed high outflow values around the right dorsolateral prefrontal cortex (DLPFC) for all ictal events; these areas coincide well with the surgical resection areas depicted in Fig. 2b. Specifically, in event numbers 1, 2, 6, 7, 12, 14, 16, 18, and 20, highly focalized outflow distributions were observed around the border among two large subdural grids and within two strips located at the prefrontal lobe. Although some spurious or widespread outflow distributions were also observed outside of the resection areas in events 3, 4, 9, 10, 11, 17, and 19, the overall distributions were not very different from the common outflow patterns, and all of them overlapped with the resection areas.

Fig. 3a shows the distributions of the outflow values for subject 2 (JMS). In this patient, 16 ictal events acquired from 100 electrodes were analyzed. The outflow distributions observed in this patient showed the most consistent pattern among those of the three LGS patients considered in the present study, with a wide distribution over the superior DLPFC and premotor cortex. None of the events showed uncommon outflow distributions. A comparison of the outflow distributions with the surgical resection areas depicted in Fig. 3b clearly demonstrates that the anterior part of the outflow distribution overlapped with the resection areas. However, we confirmed after blinded analysis that the posterior part had been also identified as a primary ictal onset zone based on other pre-surgical evaluation methods but this region had been

Author's personal copy

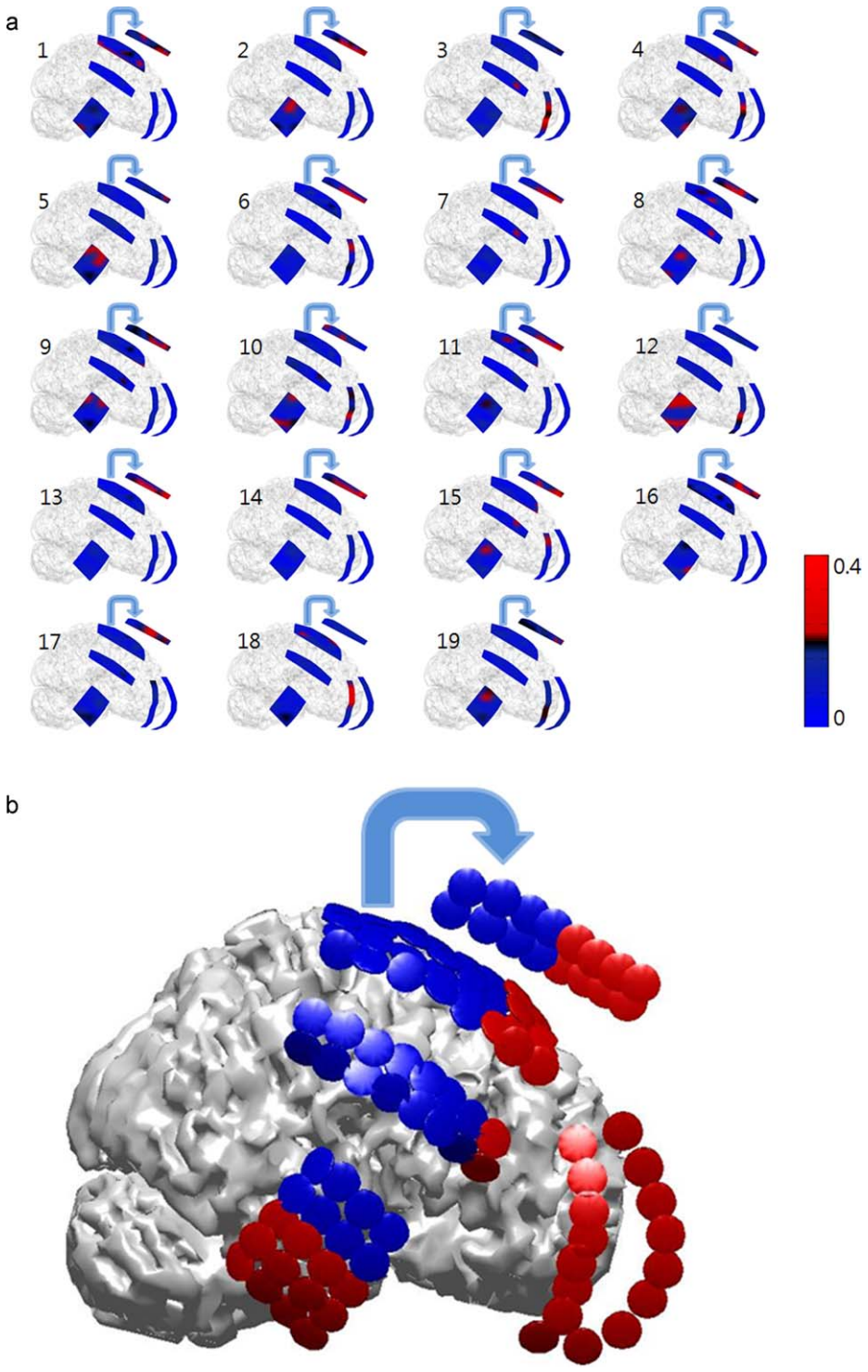

Fig. 4. The distributions of outflow values calculated for subject 3: (a) 3D outflow maps estimated for 19 ictal events. Strip electrodes implanted in the frontal medial wall are presented separately for visualization purposes; (b) the surgical resection areas (red color) marked on subdural electrodes. Numbers in (a) represent the event number. (For interpretation of the references to color in this figure legend, the reader is referred to the web version of the article.)

excluded from the final epilepsy surgery plan, as it might be associated with the patient's motor functions. Interestingly, the middle and inferior temporal gyri included in the surgical resection areas were not identified as primary ictal onset zones in the present analysis. These results suggest that activity around the temporal lobe may be propagated from another region, although we have no way to test this hypothesis. In future studies, we intend to determine the accuracy of our approach by quantitatively comparing the present results with those from different imaging modalities.

Fig. 4a shows the distributions of the outflow values for subject 3 (SWJ). The strip electrodes implanted in the frontal medial wall are presented separately. In this subject, 19 ictal events recorded from 116 electrodes were analyzed. Although the outflow distributions were not as consistent as those of subjects 1 and 2, most maps showed high outflow values around the temporal

Author's personal copy

lobe, prefrontal cortex, and medial frontal eye fields, with fairly good overlap with the surgical resection areas depicted in Fig. 4b.

4. Discussion

In the present study, we demonstrated that directional connectivity analysis of iEEG recording data can be a useful auxiliary tool for delineating surgical resection areas in LGS patients with abundant generalized epileptiform discharges.

4.1. Identification of ictal onset zones in LGS

LGS is one of the most intractable catastrophic epilepsies in children, characterized by multiple types of generalized seizures, interictal bilaterally synchronous slow spike-waves and paroxysmal fast activity in EEG, as well as progressive cognitive impairment.[15] Most patients with LGS have bilateral diffuse encephalopathy, but focal lesions that contribute to secondary generalized epileptic encephalopathy can be identified using other localized EEG findings such as persistent localized polymorphic slowings, spindle-shaped fast activities, localized paroxysmal fast activities, focal subclinical seizure activities, brief ictal rhythmic discharges, and electrodecrements.[17] In addition, recent advances in neuroimaging techniques with MRI as well as PET/SPECT could improve the detection of partial lesions.[18] Recently, Cleveland's group reported successful outcomes of resective epilepsy surgery in children with brain MRI lesions, despite abundant generalized and multiregional EEG abnormalities.[16] For ictal SPECT, we prolonged the injection of ECD during repeated brief seizures instead of using the typical rapid shooting of the tracer. Using this slow ictal SPECT protocol, we were able to detect significant SISCOM findings in the ipsilateral epileptogenic area. Furthermore, we expanded our surgical experience to include cryptogenic LGS patients without brain MRI abnormalities. Nevertheless, despite these advanced modalities, it is still difficult to correctly localize ictal onset zones in patients with LGS with abundant ictal/interictal generalized epileptiform discharges; additional refinement techniques to confirm ictal onset zones are therefore in great demand. The present study originally applied the DTF technique, which has been widely used to identify ictal onset zones in focal epilepsy, to the localization of ictal onset zones in LGS patients. The analysis results demonstrated that areas with high outflow values corresponded well with surgical resection areas identified by multiple neuroimaging modalities, suggesting that directional connectivity analysis can be used as an auxiliary tool to confirm the ictal onset zones identified using traditional neuroimaging modalities, as well as an alternative modality to determine the ictal onset zones of LGS patients.

4.2. The DTF technique as a tool for localizing ictal onset zones

Franaszczuk et al.[10] first applied the DTF technique to human iEEG data acquired from patients with mesial temporal lobe epilepsy. They recorded three patients' iEEG using a combined subdural grid and depth electrode array during complex partial seizures. They demonstrated that the patterns of seizure propagation could be identified successfully using DTF analysis. Since that study, Franaszczuk and Bergey[11] have applied the same analysis method to iEEG data acquired from patients with lateral temporal lobe epilepsy and compared the resultant propagation patterns with those of mesial temporal lobe epilepsy. Their results suggested that the DTF-based analysis of epileptic networks is a powerful technique, particularly when the patterns of seizure propagation cannot be readily identified from visual inspection of the iEEG signals.

Recently, a combinatory approach to integrate EEG source localization with the DTF method was proposed[7] to distinguish ictal onset zones from irritative zones activated by propagation of epileptiform activities. These authors used high-density scalp EEG to record ictal epileptiform activity and applied a spatiotemporal source localization method called the first principle vectors (FINEs) algorithm to extract the time series of primary and secondary source activities. The DTF method was then used to differentiate the ictal onset zones with cortical areas activated by propagations. Ding et al. applied their novel approach to five patients with focal epilepsy and demonstrated that the identified ictal onset zones coincided well with the observations from either MRI lesions or SPECT scans. Kim et al.[14] attempted to localize epileptogenic sources from ictal ECoG recordings based on Ding et al.'s[7] approach. They applied the FINEs algorithm along with the DTF method to six epilepsy patients who had undergone successful surgery and showed that the resultant 3-D ictal source locations coincided with surgical resection areas as well as conventional 2-D electrode-based source estimates.

Most recently, Wilke et al.[12] applied Franaszczuk et al.'s method[10,11] to localize generators of interictal epileptiform activity in 11 pediatric patients with neocortical extra-temporal lobe epilepsy. They confirmed that the ictal onset zones identified using the DTF method were consistent with those identified via visual review of ictal ECoG recordings by experienced electroencephalographers. Their study demonstrated that the DTF method can accurately localize the ictal onset zone, despite the rapid speed at which the epileptiform activity spreads throughout the neocortex. In another report by the same group,[13] they applied the same method to identical data sets and compared the ictal onset zones identified using the DTF method with those identified using source activity maps. Their results provided evidence suggesting that the DTF method is more accurate than are the conventional iEEG analysis methods.

The directional connectivity analysis that we performed in this study has an identical technical background to those of the previous studies listed above.[10–13] However, contrary to the previous studies that attempted to localize the epileptogenic focus in patients with focal epilepsy, we used the DTF method to identify ictal onset zones in patients with generalized epilepsy (LGS), demonstrating the feasibility of using the DTF method as a subsidiary neuroimaging modality for pre-surgical evaluation of LGS patients. In future studies, we hope to apply the present method to other types of intractable generalized epilepsies and also to investigate the accuracy of the localization of ictal onset zones by comparing the DTF results with results from existing neuroimaging modalities such as fMRI, PET, and SPECT.

In addition to the DTF technique, some new methods have been recently introduced to estimate the directional connectivity among simultaneously recorded neural signals, such as entropy transfer (or directed information transfer: DIT),[27] phase slope index (PSI),[28] and adaptive DTF (aDTF).[29] Although the DTF technique has proven to be robust to noise or constant phase disturbances,[9] the resultant directional connectivity estimates for non-stationary time series might not be as accurate as those for stationary time series, a well-known limitation of all MVAR-based methods. The new indices listed above have been proposed to address the stationary issue of the MVAR-based methods. Although the entropy transfer and PSI have demonstrated enhanced performances in estimating directional connectivity between non-stationary time series, more validation studies are needed as these methods have not been applied to the localization of ictal onset zones in epilepsy. The aDTF technique adopted adaptive MVAR modeling and showed nice performance

Author's personal copy

in localizing epileptogenic zones in some types of focal epilepsy.[29] Therefore, the applications of various connectivity measures to the localization of ictal onset zones in LGS would be an exciting topic that might provide us with a chance to obtain more accurate localization results, which we hope to explore in future studies.

Conflict of interest statement

The authors report no conflicts of interest.

Acknowledgements

This work was supported in part by the National Research Foundation of Korea (NRF) grant funded by the Korea government (MEST) (No. 2010-0015604) and in part by the Korea Research Foundation grant funded by the Korea Government (MEST, Basic Research Promotion Fund) (No. 2009-1345106765).

References

1. Krakow K, Woermann FG, Symms MR, Allen PJ, Lemieux L, Barker GJ, et al. EEG-triggered functional MRI of interictal epileptiform activity in patients with partial seizures. *Brain* 1999;**122**:1679–88.
2. Oliveira AJ, da Costa JC, Hilário LN, Anselmi OE, Palmini A. Localization of the epileptogenic zone by ictal and interictal SPECT with ^{99m}Tc-ethyl cysteinate dimer in patients with medically refractory epilepsy. *Epilepsia* 1999;**40**:693–702.
3. Kim YK, Lee DS, Lee SK, Chung CK, Chung JK, Lee MC. ^{18}F-FDG PET in localization of frontal lobe epilepsy: comparison of visual and SPM analysis. *Journal of Nuclear Medicine* 2002;**43**:1167–74.
4. Wu JY, Sutherling WW, Koh S, Salamon N, Jonas R, Yudovin S, et al. Magnetic source imaging localizes epileptogenic zone in children with tuberous sclerosis complex. *Neurology* 2006;**66**:1270–2.
5. Mars NJI, Lopes da Silva FH. EEG analysis methods based on information theory. In: Gevins AS, Remond A, editors. *Methods of analysis of brain electrical and magnetic signals: EEG handbook*. Amsterdam: Elsevier; 1987. p. 279–307.
6. Prusseit J, Lehnertz K. Stochastic qualifiers of epileptic brain dynamics. *Physical Review Letters* 2007;**98**:1–4.
7. Ding L, Worrell GA, Lagerlund TD, He B. Ictal source analysis: localization and imaging of causal interactions in humans. *NeuroImage* 2007;**34**:575–86.
8. Swiderski B, Osowski S, Cichocki A, Rysz A. Single-class SVM and directed transfer function approach to the localization of the region containing epileptic focus. *Neurocomputing* 2009;**72**:1575–83.
9. Kaminski MJ, Blinowska KJ. A new method of the description of the information flow in the brain structures. *Biological Cybernetics* 1991;**65**:203–10.
10. Franaszczuk PJ, Bergey GK, Kaminski MJ. Analysis of mesial temporal seizure onset and propagation using the directed transfer function method. *Electroencephalography and Clinical Neurophysiology* 1994;**91**:413–27.
11. Franaszczuk PJ, Bergey GK. Application of the directed transfer function method to mesial and lateral onset temporal lobe seizures. *Brain Topography* 1998;**11**:13–21.
12. Wilke C, van Drongelen W, Kohrman M, He B. Identification of epileptogenic foci from causal analysis of ECoG interictal spike activity. *Clinical Neurophysiology* 2009;**120**:1449–56.
13. Wilke C, van Drongelen W, Kohrman M, He B. Neocortical seizure foci localization by means of a directed transfer function method. *Epilepsia* 2010;**51**:564–72.
14. Kim JS, Im CH, Jung YJ, Kim EY, Lee SK, Chung CK. Localization and propagation analysis of ictal source rhythm by electrocorticography. *NeuroImage* 2010;**52**:1279–88.
15. Heiskala H. Community-based study of Lennox-Gastaut syndrome. *Epilepsia* 1997;**38**:526–31.
16. Wyllie E, Lachhwani DK, Gupta A, Chirla A, Cosmo G, Worley S, et al. Successful surgery for epilepsy due to early brain lesions despite generalized EEG findings. *Neurology* 2007;**69**:389–97.
17. Lee YJ, Kang HC, Lee JS, Kim SH, Kim DS, Shim KW, et al. Resective pediatric epilepsy surgery in Lennox-Gastaut syndrome. *Pediatrics* 2010;**125**:58–66.
18. Kim JT, Bai SJ, Choi KO, Lee YJ, Park HJ, Kim DS, et al. Comparison of various imaging modalities in localization of epileptogenic lesion using epilepsy surgery outcome in pediatric patients. *Seizure* 2009;**18**:504–10.
19. Lee YJ, Kang HC, Bae SJ, Kim HD, Kim JT, Lee BI, et al. Comparison of temporal lobectomies of children and adults with intractable temporal lobe epilepsy. *Child's Nervous System* 2010;**26**:177–83.
20. Palmini A, Najm I, Avanzini G, Babb T, Guerrini R, Foldvary-Schaefer N, et al. Terminology and classification of the cortical dysplasias. *Neurology* 2004;**62**:S2–8.
21. Eichler M. On the evaluation of information flow in multivariate systems by the directed transfer function. *Biological Cybernetics* 2006;**94**:469–82.
22. Strand ON. Multichannel complex maximum entropy (autoregressive) spectral analysis. *IEEE Transactions on Automatic Control* 1977;**22**:634–40.
23. Marple LS, Nuttall AH. Experimental comparison of three multichannel linear prediction spectral estimators. *IEE Proceedings Part F Communications Radar and Signal Processing* 1983;**130**:218–29.
24. Neumaier A, Schneider T. Estimation of parameters and eigenmodes of multivariate autoregressive models. *ACM Transactions on Mathematical Software* 2001;**27**:27–57.
25. Schlogl A. A comparison of multivariate autoregressive estimators. *Signal Processing* 2006;**86**:2426–9.
26. Schwarz G. Estimating the dimension of a model. *The Annals of Statistics* 1978;**6**:461–4.
27. Schreiber T. Measuring information transfer. *Physical Review Letters* 2000;**85**:461–4.
28. Nolte G, Ziehe A, Nikulin VV, Schlögl A, Krämer N, Brismar T, et al. Robustly estimating the flow direction of information in complex physical systems. *Physical Review Letters* 2008;**100**:1–4.
29. Wilke C, Ding L, He B. Estimation of time-varying connectivity patterns through the use of an adaptive directed transfer function. *IEEE Transactions on Biomedical Engineering* 2008;**55**:2557–64.